JBC RESEARCH ARTICLE

LncRNA *FAM83H-AS1* inhibits ferroptosis of endometrial cancer by promoting DNMT1-mediated CDO1 promoter hypermethylation

Received for publication, February 18, 2024, and in revised form, July 18, 2024 Published, Papers in Press, August 17, 2024,
https://doi.org/10.1016/j.jbc.2024.107680

Ruiyu Wang[1,2], **Xiuzhang Yu**[1,2], **Hui Ye**[1,2], **Mengyin Ao**[1,2], **Mingrong Xi**[1,2], **and Minmin Hou**[1,2,*]

From the [1]*Department of Obstetrics and Gynecology, West China Second University Hospital, Sichuan University, Chengdu, Sichuan, China;* [2]*Key Laboratory of Birth Defects and Related Diseases of Women and Children Sichuan University, Ministry of Education, Chengdu, Sichuan, China*

Reviewed by members of the JBC Editorial Board. Edited by Brian D. Strahl

Endometrial cancer (EC) is the most prevalent gynecological epithelial malignancy. DNA methylation is a promising cancer biomarker but limited use for detecting EC. We previously found that the level of cysteine dioxygenase 1 (CDO1) promoter methylation was elevated in EC patients through methylomics, but the role and mechanism of CDO1 in EC remained unclear. Here, the methylation level of CDO1 promoter was detected by bisulfite-sequencing PCR and methylation-specific PCR (bisulfite conversion-based PCR methods, which remain the most commonly used techniques for methylation detection). Cells were incubated with erastin (the ferroptosis activator). Cell vitality was measured using the cell counting kit-8 assay. *FAM83H-AS1* cellular distribution was analyzed by the fluorescence *in situ* hybridization assay. Lipid reactive oxygen species level was examined by BODIPY-C11 staining. The interactions between *FAM83H-AS1*, CDO1, and DNA methyltransferase1 (DNMT1) were analyzed by RNA-binding protein immunoprecipitation or chromatin immunoprecipitation assay. The xenograft mouse model was utilized to test CDO1 and *FAM83H-AS1*'s influence on tumor development *in vivo*. Results showed that CDO1 was hypermethylated and downregulated in EC. CDO1 knockdown reduced erastin-induced ferroptosis in EC cells. Mechanistically, DNMT1 is a DNA methyltransferase, which can transfer methyl groups to cytosine nucleotides in genomic DNA. Long noncoding RNA *FAM83H-AS1* increased CDO1 promoter methylation level and inhibited its expression in EC cells by recruiting DNMT1. CDO1 knockdown or *FAM83H-AS1* overexpression promoted EC tumor growth *in vivo*. Long noncoding RNA *FAM83H-AS1* inhibited ferroptosis in EC by recruiting DNMT1 to increase CDO1 promoter methylation level and inhibit its expression.

Endometrial cancer (EC) is a common gynecological malignancy with high morbidity and mortality rates (1). With a dismal 5-years survival rate of only 17.8%, the outlook for EC patients is still dire (2). The survival rate for EC patients has not improved considerably in recent years (3). Ferroptosis is a novel kind of Fe^{2+}-dependent programmed cell death, characterized by glutathione (GSH) consumption and lipid peroxide and reactive oxygen species (ROS) buildup, and its activation can significantly inhibit EC metastasis and recurrence and improve prognosis (4). Therefore, understanding the regulatory mechanisms of ferroptosis during EC progression may contribute to the development of novel EC treatment strategies.

Cysteine dioxygenase 1 (CDO1), a nonheme ferroenzyme involved in cysteine-to-cysteine sulfonic acid conversion, can induce ferroptosis in cancer cells by inhibiting GSH production and increasing ROS production (5). CDO1 has been identified as a ferroptosis-related gene for clinically predicting recurrence after hepatectomy of hepatocellular carcinoma patients (6). In addition, Hao *et al.* demonstrated that CDO1 inhibited gastric cancer development by mediating erastin-induced ferroptosis (5). Notably, a previous study revealed that CDO1 was a hypermethylated gene in EC patients (7). Our previous study also revealed that the methylation level of CDO1 promoter was significantly elevated in cervical scrapings from EC patients through methylomics (8). In the current study, it was predicted that *CDO1* was downexpressed in EC using the GEPIA database, but its significance in EC remained unknown. DNA methylation is one of the most common epigenetic regulatory mechanisms in mammalian cells, and its dysregulation leads to abnormal expression of tumor-related genes in various human tumors (9). DNA methylation is controlled by DNA methyltransferases (DNMTs), which include DNMT1, DNMT3A, and DNMT3B (10). DNMT1 is overexpressed in EC (11). Additionally, DNMT3A and DNMT3B overexpression may be associated with poor survival in EC patients (12). Herein, by using the methylation prediction tool (MethPrimer), it was predicted that there were CpG islands in the promoter region of CDO1. Nevertheless, the regulation mechanism of CDO1 promoter methylation in EC remains unclear, which deserves further research.

The upstream regulation mechanism of CDO1 in EC was subsequently explored. As reported, long noncoding RNAs (lncRNAs) play an important role in cancer by recruiting

* For correspondence: Minmin Hou, mminnh789@163.com.

© 2024 THE AUTHORS. Published by Elsevier Inc on behalf of American Society for Biochemistry and Molecular Biology. This is an open access article under the CC BY-NC-ND license (http://creativecommons.org/licenses/by-nc-nd/4.0/).

DNMTs to regulate the methylation of downstream genes (13). For instance, lncRNA *KCNQ1OT1* facilitated ovarian cancer metastasis by increasing the methylation of EIF2B5 promoter through recruiting DNMT1, DNMT3A, and DNMT3B (14). In addition, lncRNA *RAMP2-AS1* suppressed CXCL11 expression to inhibit the development of breast cancer by recruiting DNMT1 and DNMT3B (15). Therefore, it is speculated that lncRNA may regulate CDO1 expression in EC through DNMTs. LncRNAs are noncoding RNAs that are longer than 200 nucleotides (16). LncRNAs are key players in EC progression. For instance, lncRNA *FOXCUT* was markedly upregulated in EC cells, and its upregulation facilitated EC cell malignant behaviors (17). LncRNA *FAM83H-AS1* functions as an oncogene in various human malignant tumors. As proof, lncRNA *FAM83H-AS1* was highly expressed in cervical cancer, and its knockdown remarkably inhibited cervical cancer cell malignant behaviors (18). Additionally, *FAM83H-AS1* upregulation facilitated radio-resistance and metastasis in ovarian cancer (19). Nonetheless, the function of *FAM83H-AS1* in EC remains uncertain. In the present work, it was predicted that *FAM83H-AS1* was strongly expressed in EC using the GEPIA database, and its expression was opposite to CDO1 expression. Herein, it was observed that *FAM83H-AS1* interacted with DNMT1 protein by using RPISeq prediction. It is suggested that *FAM83H-AS1* may reduce CDO1 expression in EC by interacting with DNMT1.

Collectively, it is hypothesized that lncRNA *FAM83H-AS1* suppresses ferroptosis in EC by recruiting DNMT1 to mediate hypermethylation of the CDO1 promoter. Our study provides a theoretical foundation for the development of novel EC treatment techniques.

Results

The methylation level of CDO1 promoter was increased and its expression was reduced in EC

Our previous study found that the methylation level of CDO1 promoter was significantly elevated in cervical scrapings from EC patients through methylomics (8). In the current research, methylation-specific PCR (MSP) and bisulfite-sequencing PCR (BSP) results showed that the methylation level of CDO1 promoter was significantly elevated in EC patients (Figs. 1*A* and S1*A*). By using the GEPIA database, it was found that *CDO1* was markedly downregulated in uterine corpus endometrial carcinoma, uterine carcinosarcomas, cervical squamous cell carcinoma and endocervical adenocarcinoma, and breast invasive carcinoma (Figs. 1*B* and S1*B*). Meanwhile, CDO1 expression was lower in EC tissues than para-carcinoma tissues (Fig. 1, *C* and *D*). Meanwhile, immunohistochemistry (IHC) results revealed that CDO1 protein level was lower in EC tissues than in para-carcinoma tissues (Fig. 1*E*). EC patients were assigned into CDO1 low expression group and CDO1 high expression group according to CDO1 median level in EC patients, presented in Fig. 1*C*. Those above the median were high expression, while those below the median were low expression. EC patients with a high expression of CDO1 have higher survival rates (Fig. 1*F*). Table 1 showed the correlation between CDO1 expression and the clinical parameters of EC patients (age, histological grade, Federation of Gynecology and Obstetrics stage, Limph node metastasis, pathological type, and invasive depth). The results revealed that CDO1 expression was significantly correlated with Federation of Gynecology and Obstetrics stage, but there was no significant relationship between its expression and other characteristics. Collectively, hypermethylated CDO1 promoter might act as an important role in EC progression.

CDO1 knockdown inhibited ferroptosis in EC cells

The role of CDO1 in EC was subsequently investigated. As shown in Fig. 2*A*, the mRNA level of *CDO1* in EC cells (Ishikawa, HEC-1A, and HEC-1B) was significantly lower than in human endometrial cells, and there was no significant difference in other cells. Moreover, the protein level of CDO1 in EC cells (Ishikawa and HEC-1A) was lower than in human endometrial cells (Fig. S1*C*). Therefore, Ishikawa and HEC-1A cells were selected for subsequent experiments. CDO1 can promote ferroptosis by competitively restricting cysteine production in GSH (5) and is a tumor suppressor gene in various cancer cells (20). Herein, CDO1 knockdown was induced in EC cells combined with erastin (ferroptosis inducer) treatment to investigate the role of CDO1 in regulating ferroptosis during EC progression. EC cells were transfected sh-NC, sh-*CDO1*-1, sh-*CDO1*-2, or sh-*COD1*-3, and it was observed that sh-*CDO1*-1 transfection could significantly reduce CDO1 expression level in EC cells (Fig. S1, *D* and *E*). Therefore, sh-*CDO1*-1 was selected for the follow-up experiments. It was observed that sh-CDO1 transfection significantly decreased CDO1 expression in Ishikawa and HEC-1A cells (Fig. 2, *B* and *C*), indicating that the transfection was successful. EC cell viability was increased after CDO1 knockdown, while it was reduced by erastin treatment alone, and CDO1 knockdown weakened erastin's inhibition on EC cell viability (Fig. 2*D*). In addition, CDO1 knockdown decreased lipid ROS, malondialdehyde (MDA), and Fe^{2+} levels and increased GSH level in EC cells, while erastin treatment alone presented the opposite effects, and erastin-mediated regulation effect on these molecules was weakened by CDO1 silencing (Fig. 2, *E* and *F*). Furthermore, CDO1 knockdown increased glutathione peroxidase 4 (GPX4) and solute carrier family seven member 11 (SLC7A11) protein levels and reduced acyl-CoA synthetase long-chain family member 4 (ACSL4) and p-p38 levels in EC cells, while erastin treatment alone showed the opposite effects, and the regulation effect of erastin on the expressions of these ferroptosis-related proteins was partially reversed by CDO1 knockdown (Fig. 2*G*). All these results suggested that CDO1 silencing suppressed ferroptosis in EC cells.

LncRNA FAM83H-AS1 *inhibited CDO1 expression in EC cells by increasing CDO1 methylation level*

The regulation mechanism of CDO1 in regulating ferroptosis during EC progression was further investigated. LncRNA *FAM83H-AS1* is an oncogene in various tumors and is linked with poor prognosis (21). Using the GEPIA database, it was

ASBMB

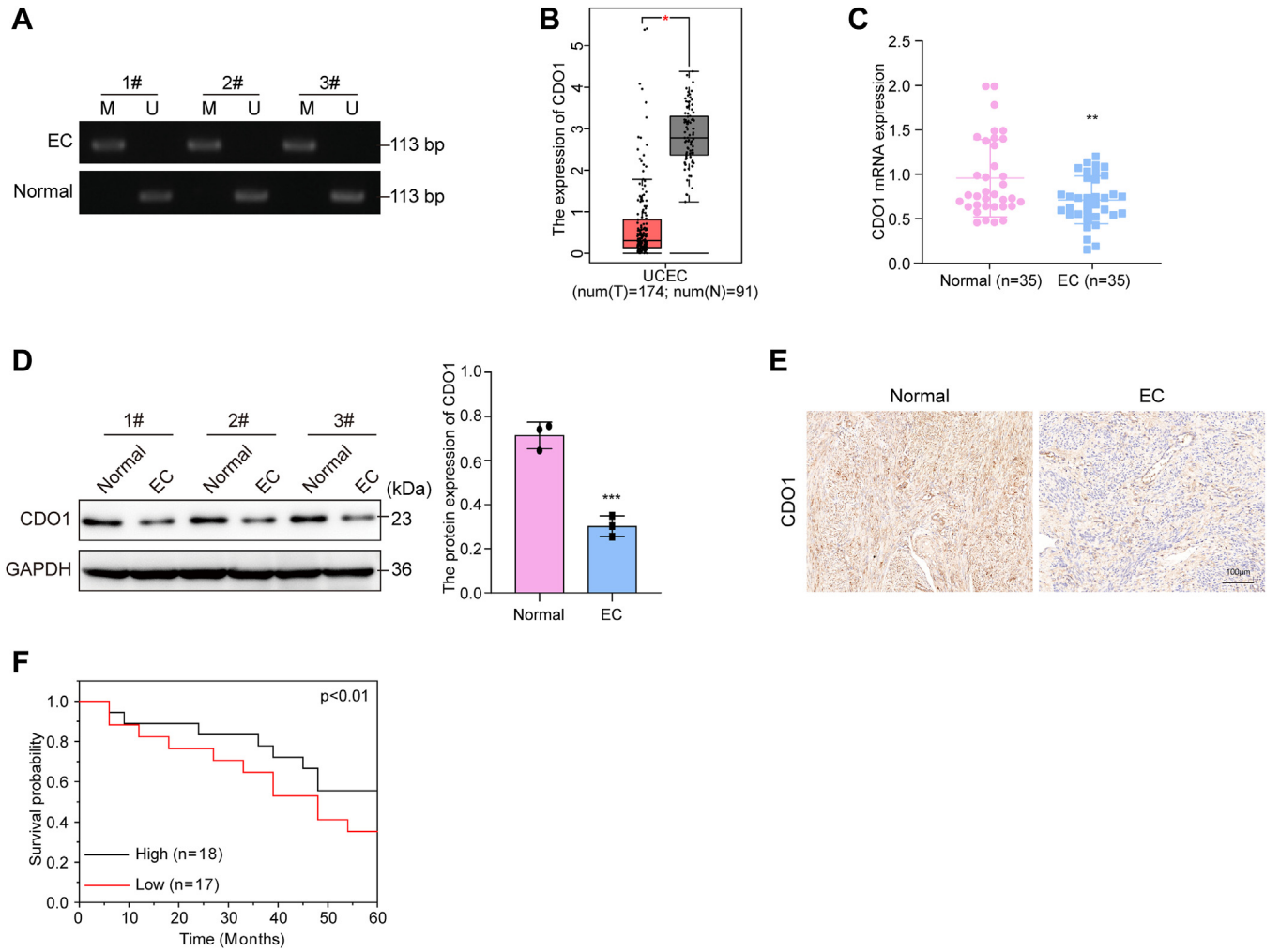

Figure 1. The methylation level of CDO1 promoter was increased while its expression was reduced in EC. A total of 35 EC tumor tissues and paired adjacent normal tissues were collected postoperatively from EC patients. *A*, the methylation level of CDO1 promoter in EC tissues and paracarcinoma tissues was examined by MSP (M: Methylation, U: Unmethylation). *B*, *CDO1* expression in UCEC was predicted by GEPIA database (T: Tumor, N: Normal). *C* and *D*, CDO1 expression levels in EC tissues and para-carcinoma tissues were detected by qRT-PCR and Western blot, Student's *t* tests were used to examine the differences between the two groups. *E*, IHC was adopted to determine CDO1 protein level in tissues, 100 μm. *F*, Kaplan–Meier plotter was utilized to evaluate the prognostic values of CDO1 in EC. n = 35. The measurement data were presented as mean ± SD. $*p < 0.05$, $**p < 0.01$, $***p < 0.001$. CDO1, cysteine dioxygenase 1; EC, endometrial cancer; IHC, immunohistochemistry; MSP, methylation-specific PCR; qRT-PCR, quantitative real-time polymerase chain reaction; UCEC, uterine corpus endometrial carcinoma.

predicted that *FAM83H-AS1* was markedly elevated in uterine corpus endometrial carcinoma, uterine carcinosarcomas, cervical squamous cell carcinoma and endocervical adenocarcinoma, and breast invasive carcinoma (Figs. 3*A* and S1*F*). Subsequently, quantitative real-time polymerase chain reaction (qRT-PCR) confirmed that *FAM83H-AS1* was highly expressed EC tissues (Fig. 3*B*). Notably, *FAM83H-AS1* expression in EC was negatively correlated with CDO1 expression (Fig. 3*C*). It was predicted that *FAM83H-AS1* was distributed in both cytoplasm and nucleus using the lncATLAS database (https://lncatlas.crg.eu/) (Fig. 3*D*), which was further confirmed by fluorescence *in situ* hybridization (Fig. 3*E*). It has been widely illustrated that lncRNA-mediated DNA methylation is a key player in cancer development (13). MethPrimer predicted the presence of CpG islands in the promoter region of CDO1 (Fig. 3*F*). The methylation sites of CDO1 were shown in Fig. S2*A*. It was observed that the methylation sites of CDO1 mainly concentrated on CpG islands, and the CpG islands of CDO1 were located on the promoter of CDO1 (Fig. S2*A*). EC cells were transfected sh-NC, sh-*FAM83H-AS*1, sh-*FAM83H-AS1*-2, or sh-*FAM83H-AS1*-3, and it was observed that sh-*FAM83H-AS*1-2 transfection could significantly reduce *FAM83H-AS1* expression level in EC cells (Fig. S2*B*). Therefore, sh-*FAM83H-AS1*-2 was selected for the follow-up experiments. MSP and BSP results subsequently displayed that *FAM83H-AS*1 knockdown reduced CDO1 promoter methylation level in EC cells (Figs. 3*G* and S2*C*). Moreover, *FAM83H-AS1* silencing enhanced CDO1 expression in EC cells (Fig. 3, *H* and *I*). Taken together, LncRNA *FAM83H-AS1* reduced CDO1 expression in EC cells by increasing CDO1 methylation level.

LncRNA FAM83H-AS1 *increased the methylation level of CDO1 promoter in EC cells by recruiting DNMT1*

DNA methylation is regulated by DNMTs, which include DNMT1, DNMT3A, and DNMT3B (10). Herein, it was observed that *DNMT1* expression was higher in EC tissues

Table 1
Association between CDO1 expression and clinicopathological characteristics of endometrial cancer patients

Clinical characteristics	N = 35	CDO1 High (N = 18)	CDO1 Low (N = 17)	*P*
Age (years)				0.7332
<55	23	12	10	
≥55	12	6	7	
Histological grade				0.1756
G1+G2	15	10	5	
G3	20	8	12	
FIGO stage				0.0354*
I+II	23	15	8	
III+IV	12	3	9	
Lymph node metastasis				0.6581
Negative	29	14	15	
Positive	6	4	2	
Pathologic type				0.4887
Endometrioid	31	13	10	
Nonendometrioid	4	5	7	
Invasive depth				0.1811
<1/2	17	11	6	
≥1/2	18	7	11	

FIGO, Federation of Gynecology and Obstetrics, *$p < 0.05$.

than in para-carcinoma tissues (Fig. 4*A*). In addition, *DNMT1* expression was positively correlated with *FAM83H-AS1* expression but negatively correlated with *CDO1* expression (Fig. 4*B*). RNA-binding protein immunoprecipitation (RIP) assay subsequently demonstrated that DNMT1 antibody could significantly enrich FAM83H-AS1, and its enrichment effect was stronger than DNMT3A and DNMT3B antibodies (Fig. 4*C*), suggesting that DNMT1 interacted with *FAM83H-AS1*. Subsequently, chromatin immunoprecipitation assay revealed that DNMT1 interacted with CDO1, while this interaction was weakened by *FAM83H-AS1* knockdown (Fig. 4*D*). Meanwhile, it was observed that DNMT1 antibody could significantly enrich CDO1 in Ishikawa and HEC-1A cells compared with IgG antibody, while this effect was weakened by sh-DNMT1 transfection (Fig. S2*D*). Ishikawa and HEC-1A cells were transfected with sh-DNMT1 or Oe-DNMT1, and it was observed that sh-DNMT1 transfection significantly reduced DNMT1 mRNA and protein levels in cells, while Oe-DNMT1 transfection markedly elevated DNMT1 mRNA and protein levels in cells (Fig. S2, *E* and *F*). CDO1 promoter methylation level was reduced by DNMT1 knockdown or *FAM83H-AS1* knockdown, which was consistent with the results of 5-Aza-dc (methyltransferase inhibitor) treatment, and DNMT1 upregulation abolished *FAM83H-AS1* knockdown's inhibition on CDO1 promoter methylation level (Figs. 4*E* and S2*G*). Finally, DNMT1 knockdown or *FAM83H-AS1* knockdown alone increased CDO1 expression level in EC cells, but DNMT1 overexpression eliminated this effect of *FAM83H-AS1* knockdown (Fig. 4, *F* and *G*). Collectively, *FAM83H-AS1* increased CDO1 methylation level and reduced CDO1 expression in EC cells by DNMT1.

LncRNA FAM83H-AS1 *regulated ferroptosis in EC cells by CDO1*

To investigate the function of *FAM83H-AS1*/CDO1 in controlling ferroptosis during EC development, *FAM83H-AS1* and CDO1 silencing were induced in DMSO/erastin-treated EC cells. It was firstly observed that CDO1 expression in EC cells was significantly increased by *FAM83H-AS1* knockdown, but CDO1 silencing weakened this change (Fig. 5, *A* and *B*). *FAM83H-AS1* knockdown reduced EC cell viability, but CDO1 silencing partially reversed this effect (Fig. 5*C*). It was also observed that *FAM83H-AS1* knockdown decreased EC cell viability under the condition of erastin existence, while CDO1 silencing increased EC cell viability and weakened the effect of sh-*FAM83H-AS1* (Fig. 5*C*). In addition, *FAM83H-AS1* downregulation increased lipid ROS, MDA, and Fe^{2+} levels and reduced GSH level in EC cells, while these sh-*FAM83H-AS1*-induced effects were all eliminated by CDO1 knockdown (Fig. 5, *D* and *E*). Meanwhile, sh-*FAM83H-AS*1 transfection elevated lipid ROS, MDA, and Fe^{2+} levels while reducing GSH level in EC cells under erastin treatment, and CDO1 silencing weakened the effects of FAM83H-AS1 silencing (Fig. 5, *D* and *E*). Moreover, *FAM83H-AS1* knockdown reduced GPX4 and SLC7A11 protein levels and increased ACSL4 and p-p38 levels in EC cells, which were partially reversed by CDO1 knockdown (Fig. 5*F*). It also turned out that *FAM83H-AS1* silencing reduced GPX4 and SLC7A11 protein levels while elevating ACSL4 and p-p38 levels in EC cells under the condition of erastin existence, and CDO1 knockdown partially eliminated these effects of *FAM83H-AS1* silencing (Fig. 5*F*). In summary, lncRNA *FAM83H-AS1* upregulation inhibited ferroptosis in EC cells by reducing CDO1 expression.

CDO1 knockdown or FAM83H-AS1 *overexpression promoted EC tumor growth* in vivo *by inhibiting ferroptosis*

The tumor implantations experiment was used to verify the effect of CDO1 and *FAM83H-AS1* on tumor growth in mice. As shown in Fig. 6, *A*–*C*, erastin treatment markedly inhibited tumor growth, while the antitumor effect of erastin was partially reversed by CDO1 knockdown or *FAM83H-AS1* overexpression. Meanwhile, IHC showed that the level of ki67 (cell proliferating marker) in tumor tissues was markedly reduced by erastin treatment, while this effect was weakened after CDO1 knockdown or *FAM83H-AS1* overexpression (Fig. 6*D*). As shown in Fig. 6, *E* and *F*, erastin treatment increased CDO1 expression in tumor tissues but did not change *FAM83H-AS1* expression significantly. CDO1 knockdown also reduced CDO1 expression but did not change *FAM83H-AS1* expression in tumor tissues, and *FAM83H-AS1* overexpression elevated *FAM83H-AS1* expression and decreased CDO1 expression in tumor tissues (Fig. 6, *E* and *F*). In addition, erastin treatment significantly elevated ROS, MDA, and Fe^{2+} levels while reducing GSH level in tumor tissues, while these effects of erastin were partially reversed by CDO1 silencing or *FAM83H-AS1* upregulation (Fig. 6*G*). Finally, erastin treatment reduced GPX4 and SLC7A11 protein levels and increased ACSL4 and p-p38 levels in tumor tissues, but CDO1 silencing or *FAM83H-AS1* upregulation weakened these alterations (Fig. 6*H*). Collectively, CDO1

ASBMB

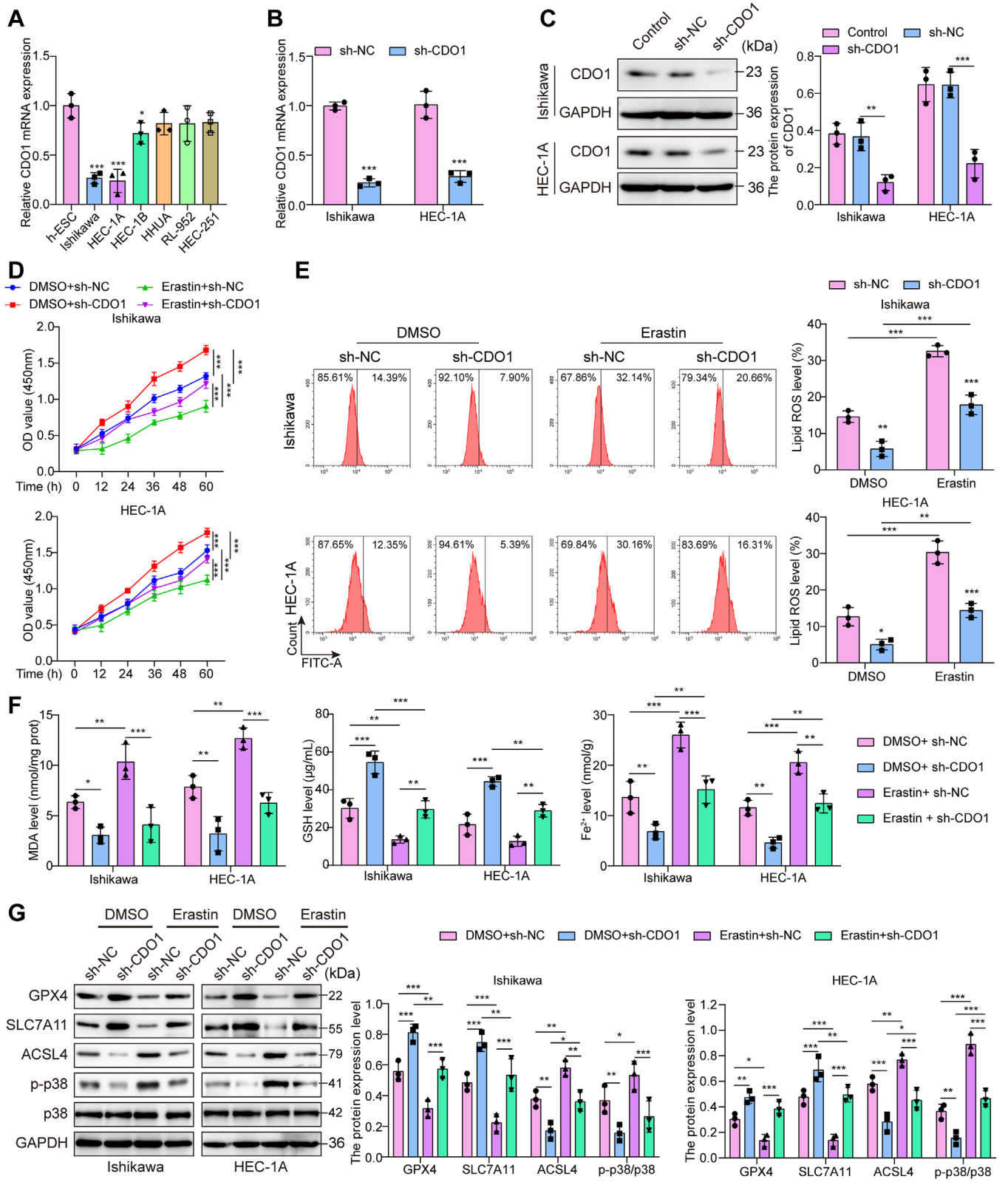

Figure 2. CDO1 knockdown inhibited ferroptosis in EC cells. *A*, qRT-PCR was employed to examine CDO1 mRNA level in EC cells (Ishikawa, HEC-1A, HEC-1B, HHUA, RL-952, and HEC-251) and human endometrial cells. EC cells were transfected with sh-NC or sh-CDO1 combined with erastin (ferroptosis inducer) treatment. *B* and *C*, CDO1 expression levels in Ishikawa and HEC-1A cells were measured by qRT-PCR and Western blot. *D*, EC cell viability was assessed by CCK-8 assay. *E*, lipid ROS level in EC cells was examined by BODIPY-C11 staining. *F*, MDA, GSH, and Fe^{2+} levels in cells were measured by the corresponding kits. *G*, Western blot was utilized to detect GPX4, SLC7A11, ACSL4, p38, and p-p38 protein levels in cells. The measurement data were presented as mean ± SD. All data were obtained from at least three independent biological replicates. The differences among multiple groups in above data were analyzed by one-way ANOVA, followed by Tukey's *post hoc* test. *$p < 0.05$, **$p < 0.01$, ***$p < 0.001$. ACSL4, acyl-CoA synthetase long-chain family member 4; CCK-8, cell counting kit-8; CDO1, cysteine dioxygenase 1; EC, endometrial cancer; GPX4, glutathione peroxidase 4; GSH, glutathione; MDA, malondialdehyde; qRT-PCR, quantitative real-time polymerase chain reaction; ROS, reactive oxygen species; SLC7A11, solute carrier family 7 member 11.

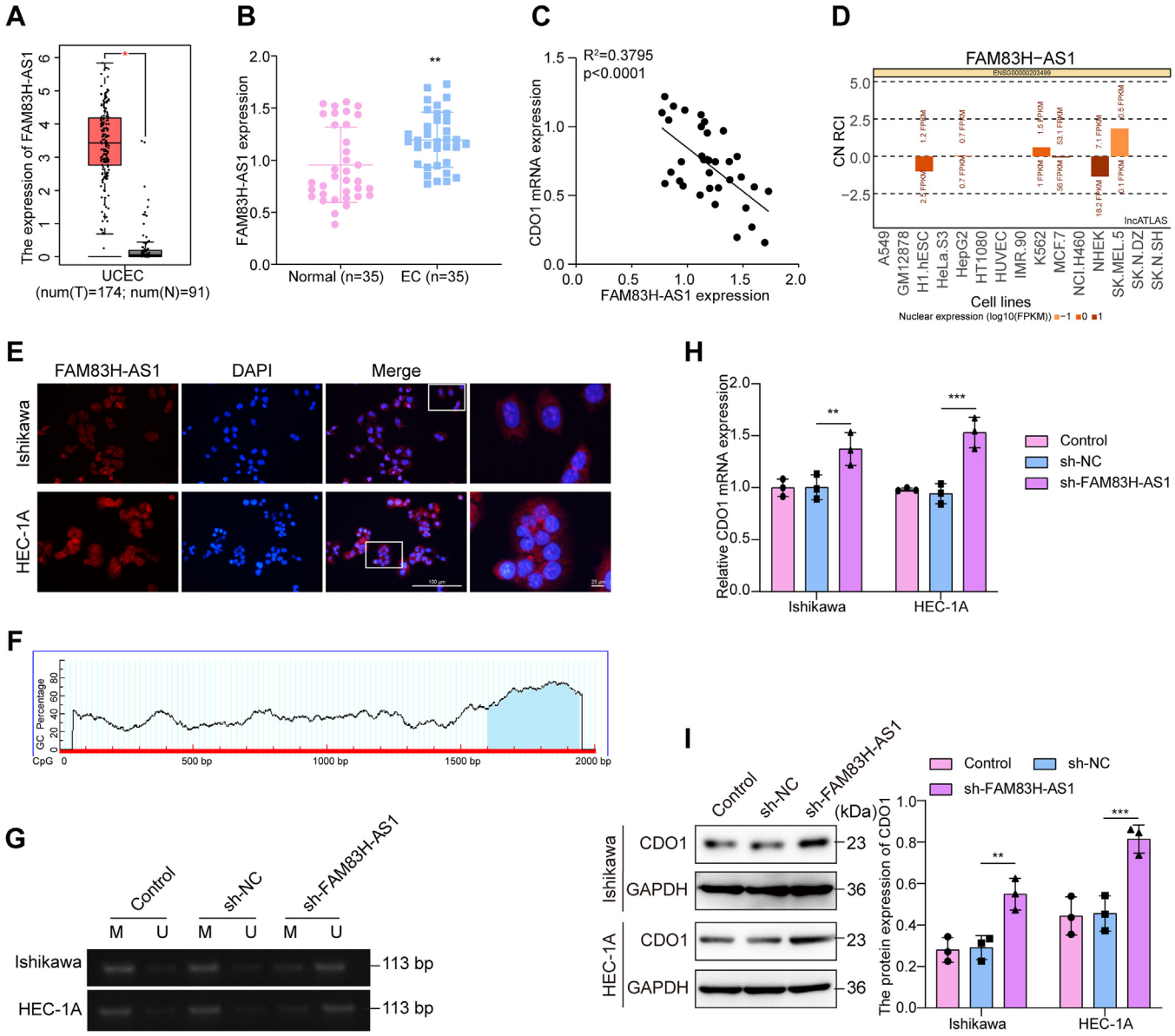

Figure 3. LncRNA *FAM83H-AS1* inhibited CDO1 expression in EC cells by increasing the methylation level of CDO1 promoter. *A*, lncRNA *FAM83H-AS1* expression in UCEC was predicted by GEPIA database. *B*, *FAM83H-AS1* expression in EC tissues and paracarcinoma tissues was detected by qRT-PCR (n = 35), Student's *t* tests were used to examine the differences between the two groups. *C*, Pearson correlation analysis (n = 35) was used to examine the relationship between *FAM83H-AS1* expression and CDO1 expression (n = 35). *D*, cellular distribution of *FAM83H-AS1* was predicted using the lncATLAS database (https://lncatlas.crg.eu/). *E*, FISH assay was adopted to analyzed cellular distribution of *FAM83H-AS1*, 100 μm and 25 μm. *F*, the existence of CpG islands in CDO1 promoter was predicted using MethPrimer. *G*, the methylation level of CDO1 promoter in EC cells following *FAM83H-AS1* silencing was examined by MSP. *H* and *I*, CDO1 expression levels in EC cells after *FAM83H-AS1* knockdown were measured by qRT-PCR and Western blot and the differences among multiple groups were analyzed by one-way ANOVA, followed by Tukey's *post hoc* test. The measurement data were presented as mean ± SD. All data were obtained from at least three independent biological replicates. $^{*}p < 0.05$, $^{**}p < 0.01$, $^{***}p < 0.001$. CDO1, cysteine dioxygenase 1; EC, endometrial cancer; FISH, fluorescence in situ hybridization; MSP, methylation-specific PCR; qRT-PCR, quantitative real-time polymerase chain reaction; UCEC, uterine corpus endometrial carcinoma.

knockdown or *FAM83H-AS1* overexpression could promote EC tumor growth *in vivo* by inhibiting ferroptosis.

Discussion

EC is the most common gynecologic cancer with high mortality and recurrence rates (22). EC has a high risk of recurrence or metastasis, and the prognosis of these EC patients is not optimistic (2). Therefore, it is crucial to develop novel therapy approaches for EC. Ferroptosis is a key player in EC progression (23). Activating ferroptosis in EC cells is a potential treatment strategy for EC. Our findings show that lncRNA *FAM83H-AS1* inhibits ferroptosis in EC by recruiting DNMT1 to mediate hypermethylation of the CDO1 promoter.

The nonheme iron enzyme CDO1, which turns cysteine into cysteine sulfinic acid, is a tumor suppressor in multiple cancer cells (20). DNA methylation is a stable modification and is considered a promising marker of in research on cancer (24). Notably, our previous research demonstrated that CDO1

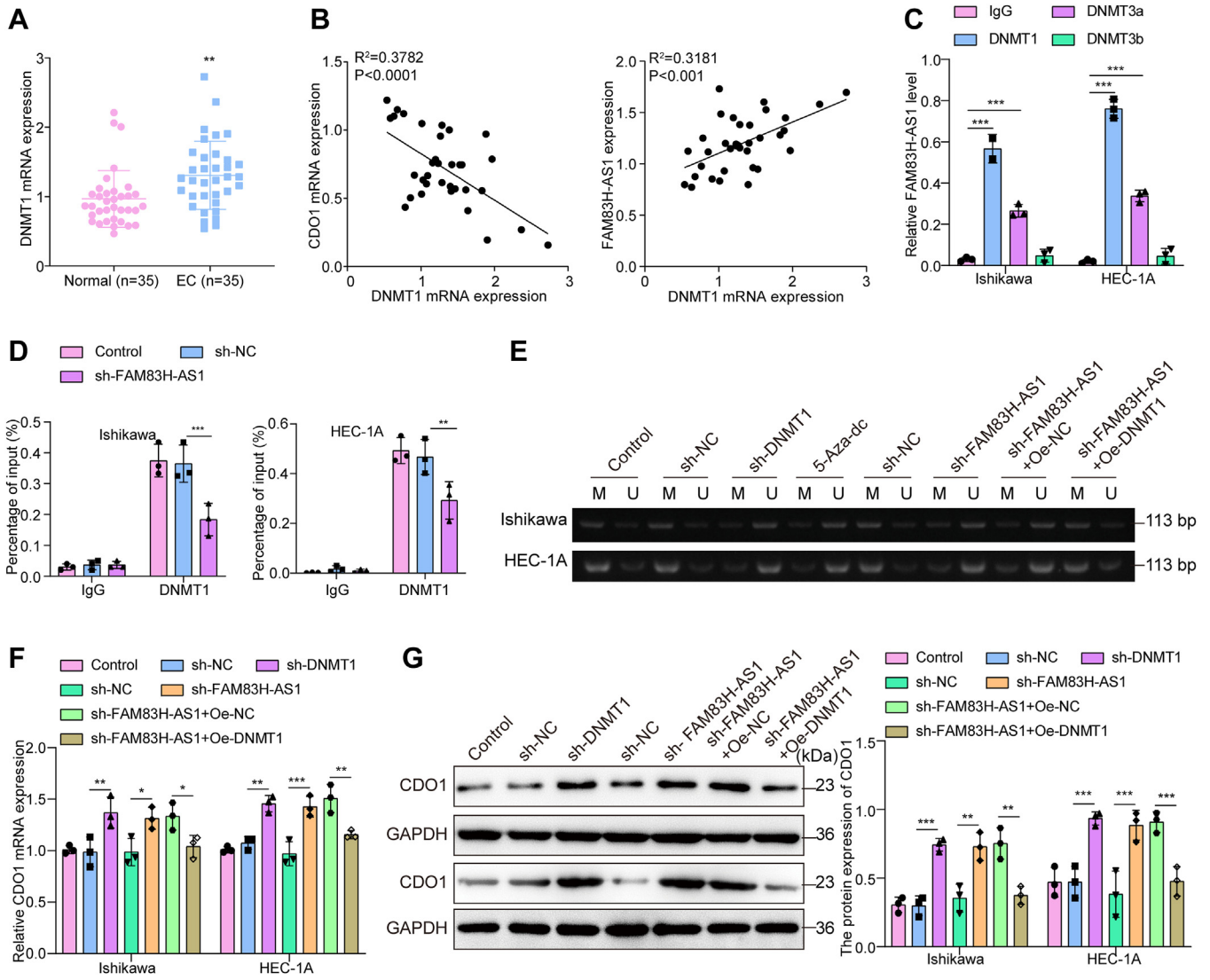

Figure 4. LncRNA *FAM83H-AS1* increased the methylation level of CDO1 promoter in EC cells by recruiting DNMT1. *A*, *DNMT1* mRNA level in EC tissues and paracarcinoma tissues was examined using qRT-PCR (n = 35), Student's *t* tests were used to examine the differences between the two groups. *B*, Pearson correlation analysis was used to examine the relationships between *DNMT1* expression, *FAM83H-AS1* expression, and CDO1 expression (n = 35). *C*, the interactions between *FAM83H-AS1* and DNA methyltransferases (DNMT1, DNMT3a, and DNMT3b) were analyzed by RIP assay. *D*, the interaction between DNMT1 and CDO1 was analyzed by ChIP assay. *E*, the methylation level of CDO1 promoter in EC cells was examined by MSP. *F* and *G*, CDO1 expression levels in EC cells were measured by qRT-PCR and Western blot. The measurement data were presented as mean ± SD. All data were obtained from at least three independent biological replicates. The differences among multiple groups were analyzed by one-way ANOVA, followed by Tukey's *post hoc* test (*C*–*G*). *$p < 0.05$, **$p < 0.01$, ***$p < 0.001$. CDO1, cysteine dioxygenase 1; ChIP, chromatin immunoprecipitation; DNMT1, DNA methyltransferase 1; EC, endometrial cancer; MSP, methylation-specific PCR; qRT-PCR, quantitative real-time polymerase chain reaction; RIP, RNA-binding protein immunoprecipitation.

promoter was hypermethylated in cervical scrapings from EC patients through methylomics (8). Consistently, it was found that the methylation level of CDO1 promoter was significantly increased in EC, while its expression was reduced. As reported, CDO1 can activate ferroptosis, and its knockdown inhibited ferroptosis in gastric cancer cells (20). However, the role of CDO1 in regulating ferroptosis during EC development remains unclear. Our experimental data showed that CDO1 knockdown inhibited erastin-induced ferroptosis in EC cells and increased EC cell viability. Meanwhile, CDO1 knockdown promoted EC tumor growth *in vivo* by inhibiting ferroptosis. This study mainly explored the mechanism of CDO1 in EC and ferroptosis, so EC cells were treated with ferroptosis inducer (Erastin). Considering that the methylation level of CDO1 promoter in EC was increased while the gene expression was decreased, it was speculated that CDO1 may act as a tumor suppressor gene in EC, and the relationship with ferroptosis in EC may be positive. In order to better explore the relationship between CDO1 and ferroptosis during EC progression, we chose to knock down CDO1 expression in EC cells combined with Erastin treatment. The p38 mitogen-activated protein kinase pathway activation induces ferroptosis in EC cells (25). Our results displayed that CDO1 knockdown ameliorated erastin-induced increase in p-p38

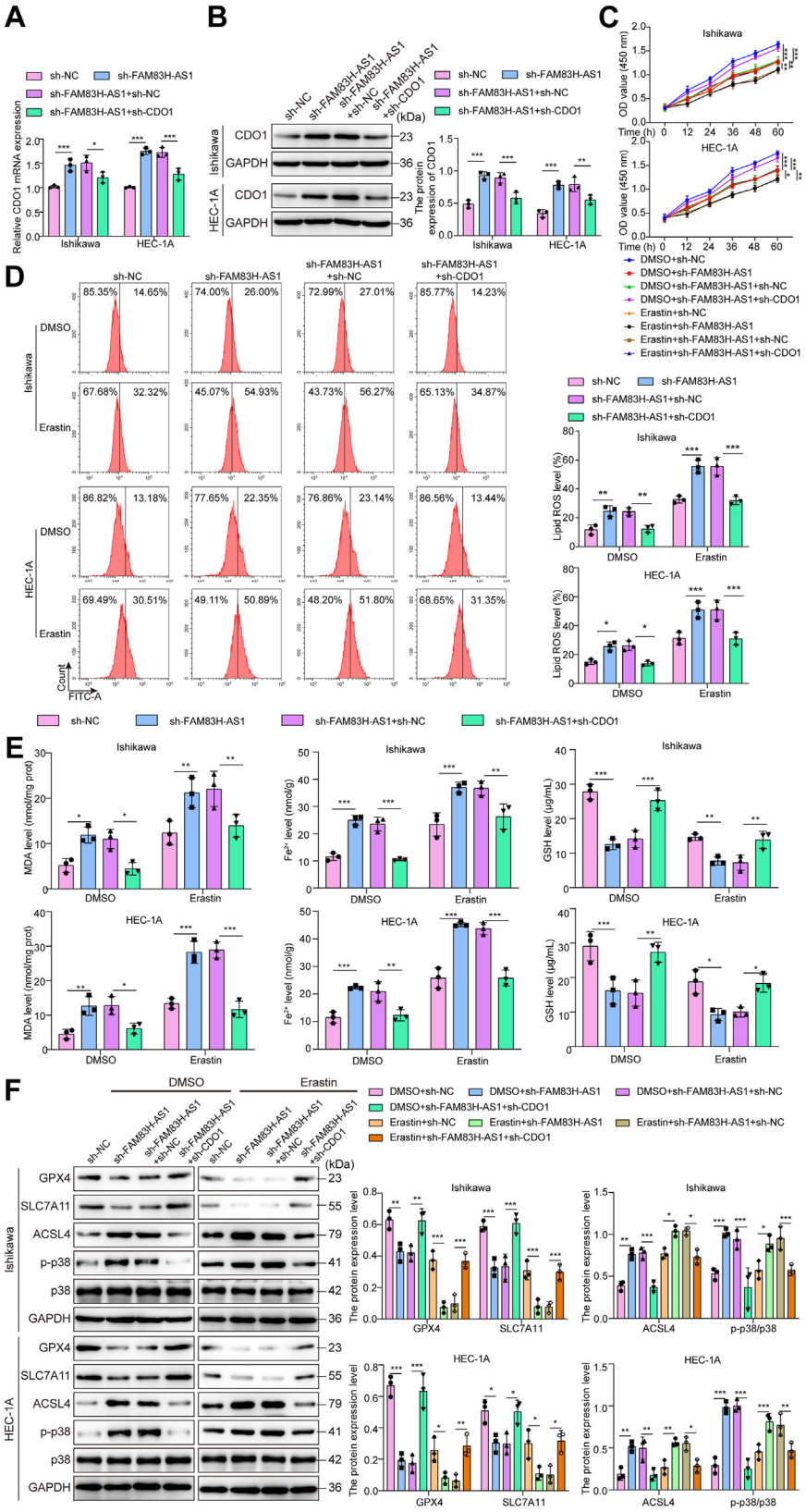

Figure 5. LncRNA *FAM83H-AS1* reduced ferroptosis in EC cells by acting on CDO1. *A* and *B*, both *FAM83H-AS1* knockdown and CDO1 knockdown were induced in EC cells, and CDO1 expression levels in cells were examined by qRT-PCR and Western blot. Both *FAM83H-AS1* knockdown and CDO1 knockdown were induced in DMSO/erastin-treated EC cells. *C*, CCK-8 assay was performed to detect EC cell viability. *D*, lipid ROS level in EC cells was examined by BODIPY-C11 staining. *E*, MDA, GSH, and Fe^{2+} levels in cells were measured by the corresponding kits. *F*, Western blot was utilized to detect GPX4, SLC7A11, ACSL4, p38, and p-p38 levels in cells. The measurement data were presented as mean ± SD. All data were obtained from at least three independent biological replicates. The differences among multiple groups in above data were analyzed by one-way ANOVA, followed by Tukey's *post hoc* test. *$p < 0.05$,

level in EC cells. Collectively, CDO1 was hypermethylated and lowly expressed in EC, and its knockdown inhibited erastin-induced ferroptosis in EC cells by inactivating the p38 mitogen-activated protein kinase pathway.

The upstream regulation mechanism of CDO1 in EC was further investigated. As widely illustrated, lncRNAs achieve their roles in diseases by regulating the methylation level of downstream target through interacting with DNMTs. For example, lncRNA *NEAT1* promoted lung cancer cell malignant phenotypes by inhibiting p53 expression through interacting DNMT1 (26). Therefore, it was speculated that lncRNA could regulate the methylation level of CDO1 promoter by recruiting DNMT1. LncRNAs have important roles in carcinogenesis. For instance, lncRNA *THOR* upregulation increased EC cell proliferation, migration, and invasion (27). In several human malignant tumors, lncRNA *FAM83H-AS1* has a carcinogenic function (28, 29). However, the expression and significance of *FAM83H-AS1* in EC are unknown, which deserves further study. Our findings showed *FAM83H-AS1* was overexpressed in EC tissues, and its overexpression promoted EC tumor growth in mice by inhibiting ferroptosis. Our results further showed that lncRNA *FAM83H-AS1* inhibited CDO1 expression in EC cells by increasing the methylation level of CDO1 promoter. The mechanism of *FAM83H-AS1* regulating CDO1 promoter methylation level was investigated. DNMT1 is a key enzyme for genome-wide DNA methylation maintenance and gene silencing (30). DNMT1 is highly expressed in multiple malignancies, and DNMT1 inhibitors have a strong potential for use in cancer therapy (31, 32). DNMT1 was shown to be substantially expressed in EC, according to our findings. DNA methylation generally occurs at the CpG island, which is rich in cytosine, phosphate, and guanine (33). After being catalyzed by DNMT, cytosine in the CpG island is converted to 5-methylcytosine, thereby inhibiting gene expression (34). It can be inferred that the interaction sites between DNMT1 and CDO1 are mainly located in the CpG island of the CDO1 promoter. Through complementary pairing, we found that the CCGCAGGGTC site in the CpG island of the CDO1 promoter is complementary to the CDS of DNMT1. Therefore, we preliminarily speculated that CCGCAGGGTC may be one of the interaction sites between DNMT1 and CDO1, but the specific content still needs further verification in the future. More importantly, *FAM83H-AS1* increased CDO1 methylation level in EC cells by interacting with DNMT1. There have been reports that multiple lncRNAs can recruit DNMTs and regulate target gene expression, thereby playing important roles in various cancers and diseases (13). It is worth noting that the possible mechanism of lncRNA recruitment for DNMT is as follows: (a) LncRNA directly recruits DNMT/TET; (b) lncRNA indirectly recruits DNMT through EZH2/PHB2; (c) lncRNA indirectly recruits TET through GADD45A. (d) lncRNA isolates DNMT; and (e) lncRNAs control SAM/SAH levels by interacting with MAT or SAHH, thereby affecting DNMT activity. In summary, the mechanisms by which lncRNA recruits DNMTs are diverse. The specific relationship between *FAM83H-AS1* and DNMT1 has not been deeply explored in this paper, but we will further explore it if future conditions permit. Moreover, *FAM83H-AS1* also recurs DNMT1 to other azacytidine sensitive genetic loci. A previous study showed that lncRNA *HOTAIR* affected the development of colorectal cancer by regulating Bcl-2 methylation through recruiting DNMT1 (35). It was also reported that lncRNA *HOTAIR* affected the development of chronic myeloid leukemia by regulating PTEN methylation through recruiting DNMT1 (36). Moreover, lncRNA *HOTAIR* affected drug resistance in small cell lung cancer cells by regulating HOXA1 methylation through recruiting DNMT1 and DNMT3b (37). It can be inferred that lncRNA *HOTAIR* can affect the methylation of multiple target genes by recruiting DNMT1. It is speculated that *FAM83H-AS1* can also recruit DNMT1 to influence other gene methylation. It is worth noting that our research group obtained CDO1 through methylation sequencing screening in the early stage, so the focus of this article is on CDO1. If future conditions permit, we will further investigate the recruitment of DNMT1 by *FAM83H-AS1* and its impact on the methylation of other genes.

Taken together, our experimental data suggested that lncRNA *FAM83H-AS1* inhibited ferroptosis in EC cells by interaction with DNMT1 to increase the methylation level of CDO1 promoter (Graphical abstract). Our research provides a theoretical foundation for creating novel EC diagnostic and treatment options.

Experimental procedures

Clinical sample collection

A total of 35 EC tumor specimens and matched surrounding normal tissues were obtained from EC patients postoperatively at West China Second University Hospital. The EC patients were diagnosed by pathology and were not treated. All samples were stored at −80 °C. Based on the median expression value, all cases of EC were divided into two groups: those with low CDO1 expression (n = 18) and those with high CDO1 expression (n = 17). The basic information was shown in Table 1. Kaplan–Meier plotter was used to assess the prognostic significance of CDO1 in EC. This study was approved by the review of Ethics Committee of West China Second University Hospital, and all participants signed informed consent. Human studies abided by the Declaration of Helsinki principles.

Immunohistochemistry

The tumor sections were heated at 60 °C and deparaffinized in xylene and gradient alcohol solutions. Then, the sections were placed in a repair box filled with citric acid antigen repair

$^{**}p < 0.01$, $^{***}p < 0.001$. ACSL4, acyl-CoA synthetase long-chain family member 4; CCK-8, cell counting kit-8; CDO1, cysteine dioxygenase 1; EC, endometrial cancer; GPX4, glutathione peroxidase 4; GSH, glutathione; MDA, malondialdehyde; qRT-PCR, quantitative real-time polymerase chain reaction; ROS, reactive oxygen species; SLC7A11, solute carrier family 7 member 11.

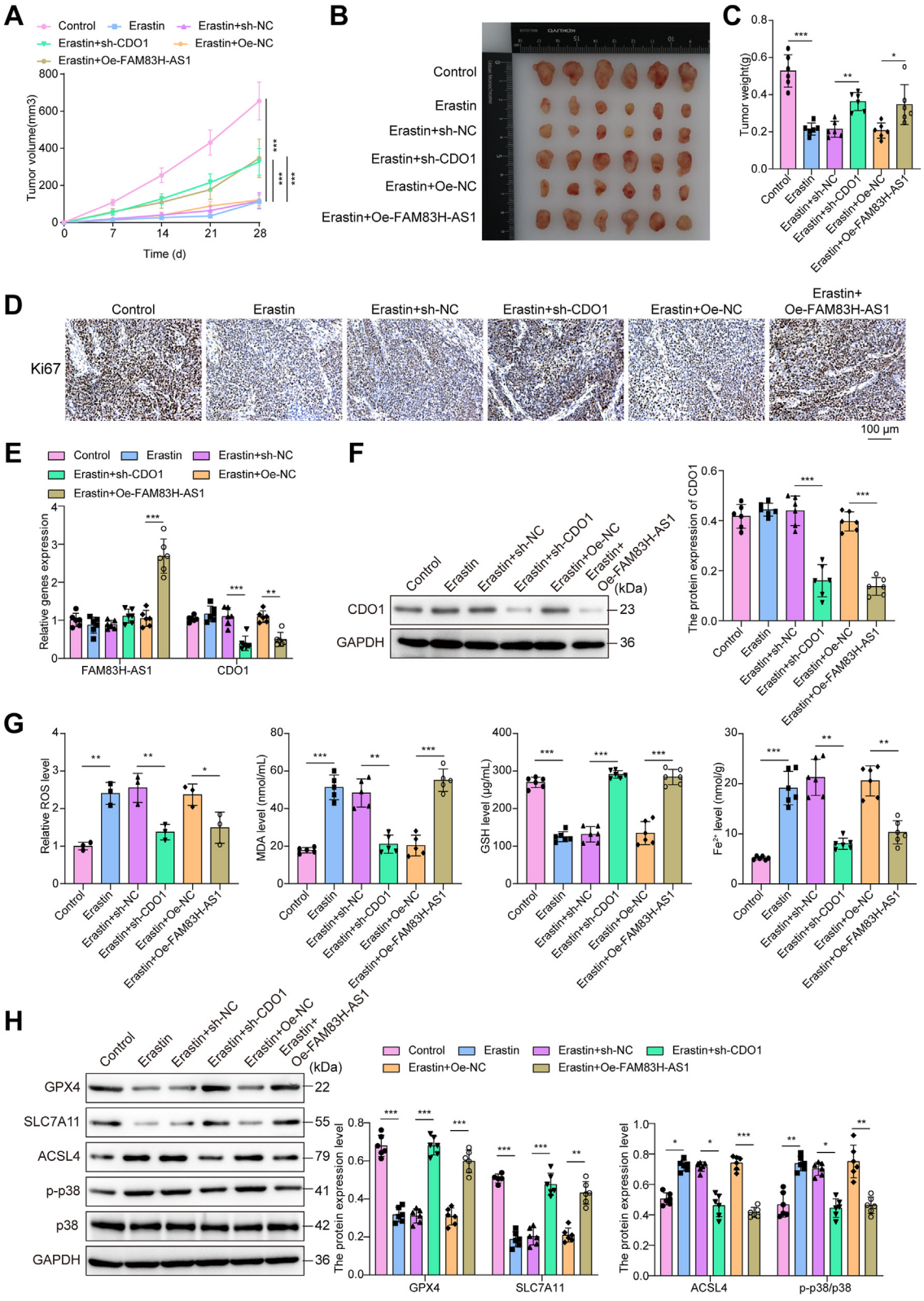

Figure 6. CDO1 knockdown or *FAM83H-AS1* overexpression inhibited EC tumor growth *in vivo* by inhibiting ferroptosis. Nude mice were injected with stable sh-CDO1 or Oe-*FAM83H-AS1* EC cells and treated with erastin meanwhile. *A–C*, tumor tissues were collected, and tumor volume and weight were measured. *D*, IHC was adopted to detect ki67 level in tumor tissues, 100 μm. *E*, *FAM83H-AS1* and CDO1 expressions in tumor tissues were determined by qRT-PCR. *F*, Western blot was utilized to analyze CDO1 level in tumor tissues. *G*, ROS, MDA, GSH, and Fe^{2+} levels in tumor tissues were measured by the corresponding kits. *H*, Western blot was used to detect GPX4, SLC7A11, ACSL4, p38, and p-p38 levels in tumor tissues. The measurement data were presented as mean ± SD. n = 6. The differences among multiple groups in above data were analyzed by one-way ANOVA, followed by Tukey's *post hoc* test. *$p < 0.05$, **$p < 0.01$, ***$p < 0.001$. ACSL4, acyl-CoA synthetase long-chain family member 4; CDO1, cysteine dioxygenase 1; EC, endometrial cancer; GPX4, glutathione peroxidase 4; GSH, glutathione; IHC, immunohistochemistry; MDA, malondialdehyde; qRT-PCR, quantitative real-time polymerase chain reaction; ROS, reactive oxygen species; SLC7A11, solute carrier family 7 member 11.

solution (pH 6.0) for antigen retrieval and incubated in a 3% hydrogen peroxide solution at room temperature in the dark for 25 min. The tumor sections were then blocked with 3% BSA for 30 min and incubated overnight with antibody against CDO1 (Abcam, 1:200, ab232699). The next day, the sections were incubated with a corresponding secondary antibody (Abcam, 1:500, ab150077) for 1 h. The slices were stained with diaminobenzidine, dried, and mounted after being counterstained with hematoxylin. The photographs were obtained with a Nikon microscope.

Cell culture and treatment

Human endometrial cells and EC cells (Ishikawa, HEC-1A, HEC-1B, HHUA, RL-952, and HEC-251) were obtained from ATCC. All cells were identified by short tandem repeats and *Mycoplasma* fluorescence quantitative PCR. Cell lines were free from *mycoplasma* contamination for all experiments. All cells were cultured in Dulbecco's modified Eagle's medium (Gibco) containing 10% FBS (Gibco) with 5% CO_2 at 37 °C. To induce ferroptosis, cells were treated with erastin (10 μM, Medchemexpress) for 24 h according to the previous report (38). All cells were authenticated by STR analysis.

Cell transfection

The short-hairpin RNAs (sh-*CDO1*-1-3, sh-*FAM83H-AS1*, and sh-*DNMT1*), the overexpression plasmid of *DNMT1* (Oe-*DNMT1*), Oe-*FAM83H-AS1*, and negative controls were purchased from GenePharma. Cells were transfected the shRNAs and vectors using Lipofectamine 3000 (Invitrogen).

sh-*CDO1*-1: GCAGCAGTATTCATGATCATA;
sh-*CDO1*-2: CGAGTAGAGAACATCAGCCAT;
sh-*CDO1*-3: GCCATGCCTTTGATCAAAGAA;
sh-*FAM83H-AS1*: GCTGTACCGTGCAGCCTTTGG;
sh-*DNMT1*: GAATCTCTTGCACGAATTTCT.

Cell counting kit-8 assay

Cells were cultured in 24-well plates (2×10^4 cells/well) for 24 h and incubated with 10 μl of Cell counting kit-8 solution at 37 °C for 3 h. The absorbance at 450 nm was measured.

Measurement of lipid ROS

Cells were seeded at a density of 4×10^4 cells/well in 24-well plates and subjected to corresponding treatments. Cells were washed and stained with 5 μM BODIPY C-11 (Thermo Fisher Scientific) in Dulbecco's modified Eagle's medium for 15 min at 37 °C. Cells were subsequently collected, washed, and resuspended in PBS. The samples were immediately analyzed by flow cytometry (BD). The populations were analyzed with FlowJo software (BD).

Measurement of Fe^{2+}, GSH, and MDA levels

Fe^{2+}, GSH, and MDA levels were examined using the Fe^{2+} assay kit (MAK025, Sigma-Aldrich), GSH assay kit (A006-2-1, Nanjing Jiancheng), and MDA assay kit (A003-1-2, Nanjing Jiancheng). All operations were strictly carried out in accordance with the manufacturer's instructions.

Fluorescence in situ hybridization

Cells were fixed, permeabilized, and blocked. Cells were then prehybridized at 37 °C for 30 min. Cells were hybridized with the lncRNA FISH Probe Mix (Ribio) overnight. Cells were washed, and the nucleus was stained using DAPI (Sangon). The images were captured using the confocal laser scanning microscopy (Carl Zeiss Microimaging).

MSP and BSP

The genomic DNAs were isolated using a Tiangen DNA extraction kit and then bisulfite-modified. The primers for methylation and unmethylation of CDO1 were synthesized. For PCR, the MSP reaction system (Takara) was utilized, which included a template, primer, PCR buffer, dNTP, and DNA polymerase. MSP products were analyzed by gel electrophoresis. The primers for methylation and unmethylation of CDO1 were listed as follows:

Left M primer TTTGGGACGTCGGAGATAAC,
Right M primer CCAAAAAAAATAACGAAAACGAA,
Left U primer GATTTTTGGGATGTTGGAGATAAT,
Right U primer ACCCAAAAAAAATAACAAAAAA CAAA.

To perform BSP, the modified DNAs were amplified, purified, subcloned into pMD19-T vector (Takara), and transformed into *E. coli* (Biowit). *E. coli* was grown in LB medium (Thermo Fisher Scientific) with 50 μg/ml ampicillin at 37 °C with 0.04% CO_2. Finally, five isolated colonies were picked and sequenced for BSP detection using an ABI 3730 DNA Sequencer (Thermo Fisher Scientific). The methylation level of the CDO1 promoter is quantitatively calculated by the following formula: black solid dots/(black solid dots + white hollow dots).

RIP assay

RIP assay was performed using the MagnaRIP RIP Kit (Millipore) according to the manufacturer's instruction. The total mRNA was isolated from cells and incubated with DNMT1 antibody (Abcam, 1:20, ab92314), DNMT3a antibody (Abcam, 1:30, ab307503), DNMT3b antibody (Abcam, 1:100, ab227883) or IgG antibody (Abcam, 1:100, ab109489), and protein A/G magnetic beads for 1 h. RNA was isolated and analyzed using qRT-PCR.

Chromatin immunoprecipitation assay

Cells were fixed and quenched. DNA was fragmented by sonication. The cell lysates were then incubated with anti-DNMT1 (Abcam, 1:100, ab92314) or anti-IgG (Abcam, 1:100, ab172730) overnight at 4 °C. Protein A/G PLUS Agarose (Santa Cruz) was used to isolate chromatin–antibody complexes. DNA was purified and analyzed using qPCR. The primer used was listed as follows:

F-CGACCCTTTTTGTCTACGTCCCA and
R-GCTTGGAGTCACTAGGAATG.

Table 2
The primer sequences of qRT-PCR in study (5′-3′)

Gene	Forward	Reverse
CDO1	CGAGTAGAGAACATCAGCCATACG	CCGAAGTTGCATTTGGAGTTCT
FAM83HAS1	CGAGGACAGCTACGGGAACAC	CGAAAGCGCCCTTGCTGTT
GAPDH	CTGACTTCAACAGCGACACC	GTGGTCCAGGGGTCTTACTC

Xenograft mouse model

BALB/c nude mice (8-week-old) were purchased from SJA LABORATORY Animal Co, Ltd. After acclimation for 1 week, mice were randomly classified into six groups: control, Erastin, Erastin + sh-NC, Erastin + sh-CDO1, Erastin + Oe-NC, and Erastin + Oe-*FAM83H-AS1*, with six animals in each group. BALB/C nude mice were subcutaneously injected with 0.2 ml PBS containing 2×10^4 Ishikawa cells which were stable transfected with Oe-NC, Oe-*FAM83H-AS1*, sh-NC, or sh-CDO1. The tumor volume was calculated using the following formula: $V = lw^2/2$ (l: the length of the tumor, w: the width of the tumor). After 1 week, mice were intraperitoneally injected with erastin (MedChemExpress, 20 mg/kg dissolved in 20 μl DMSO + 130 μl corn oil) or DMSO and corn oil mixture (20 μl DMSO + 130 μl corn oil) every 2 days for 20 days. The mice were then euthanized, and the tumor tissues were collected. IHC was used to analyze Ki67 level in tumor tissues with ki67 antibody (Abcam, 1:200, ab15580). All animal experiments were operated in accordance with the "Laboratory Animal Management Treaty" and were approved by West China Second University Hospital.

Quantitative real-time polymerase chain reaction

The total RNA was extracted with TRIzol (Beyotime). The extracted RNA was reversely transcribed using the reverse transcriptase kit (Toyobo). qRT-PCR was performed using SYBR (Thermo Fisher Scientific). GAPDH was used as the internal reference. The data were analyzed by the $2^{-\Delta\Delta CT}$ method. The primers used in the study are shown in Table 2.

Western blot

The proteins were isolated using RIPA (Beyotime) and quantified by a BCA kit (Beyotime). The total protein (20 μg) was separated using 10% SDS-PAGE and transferred to a Millipore PVDF membrane. The membranes were then blocked and incubated with antibodies against GPX4 (Abcam, 1:1000, ab125066), SLC7A11 (Abcam, 1:1000, ab307601), ACSL4 (Abcam, 1:1000, ab205199), CDO1 (Abcam, 1:1000, ab232699), p38 (Abcam, 1:1000, ab170099), p-p38 (Abcam, 1:1000, ab195049), DNMT1 (Abcam, 1:1000, ab188453), and GAPDH (Abcam, 1:5000, ab8245) overnight. The membranes were subsequently incubated with the secondary antibody (Abcam, 1:5000, ab7090) for 60 min. All antibodies were purchased from Abcam and diluted with the appropriate dilution. The blots were visualized by the GEL imaging system (Bio-Rad). The quantitative analysis of gray values was performed using Image J software (NIH).

Statistical analysis

All data were obtained from at least three independent biological replicates. SPSS 19.0 (IBM) was used to examine the statistical data. All data were presented as mean ± SD. The Shapiro–Wilk test was then utilized to assess the normality of the experimental data. All data did not deviate significantly from normality considering the 5% significance level. Unpaired Student's *t* tests were used to examine the differences between the two groups. The differences among multiple groups were analyzed by one-way ANOVA, followed by Tukey's *post hoc* test. EC patients were assigned into CDO1 low-expression group and CDO1 high-expression group according to CDO1 median level in EC patients. Those above the median were high expression, while those below the median were low expression. Kaplan–Meier method was used to analyze the effect of CDO1 on the prognosis of EC patients. The *p* values less than 0.05 were regarded as significant.

Ethics approval and consent to participate

This study was passed the review of Ethics Committee of West China Second University Hospital, and all participants signed informed consent. The animal studies were approved by West China Second University Hospital.

Data availability

The datasets generated during and/or analyzed during the current study are available from the corresponding author on reasonable request.

Supporting information—This article contains supporting information.

Author contributions—R. W. writing—original draft; R. W. methodology; R. W. conceptualization; X. Y. resources; X. Y. data curation; M. X. visualization; M. X. supervision; M. H. writing—review & editing; M. H. funding acquisition; H. Y. validation; H. Y. formal analysis; M. A. project administration; M. A. investigation.

Funding and additional information—This work was supported by grants from Clinical Research Fund of West China Second Hospital of Sichuan University (KL104) and Terahertz Science and Technology Key Laboratory of Sichuan Province (THZSC202301).

Conflicts of interest—The authors declare that there is no conflict of interest with the contents of this article.

Abbreviations—The abbreviations used are: ACSL4, acyl-CoA synthetase long-chain family member 4; BSP, bisulfite sequencing, PCR; CCK-8, cell counting kit-8; CDO1, cysteine dioxygenase 1; ChIP, chromatin immunoprecipitation; DNMT1, DNA

methyltransferase 1; EC, endometrial cancer; FISH, fluorescence *in situ* hybridization; GPX4, glutathione peroxidase 4; GSH, glutathione; IHC, immunohistochemistry; lncRNAs, long noncoding RNAs; MDA, malondialdehyde; MSP, methylation-specific PCR; qRT-PCR, quantitative real-time polymerase chain reaction; RIP, RNA-binding protein immunoprecipitation; ROS, reactive oxygen species; SLC7A11, solute carrier family 7 member 11.

References

1. Sung, H., Ferlay, J., Siegel, R. L., Laversanne, M., Soerjomataram, I., Jemal, A., *et al.* (2021) Global cancer statistics 2020: GLOBOCAN estimates of incidence and mortality worldwide for 36 cancers in 185 countries. *CA Cancer J. Clin.* **71**, 209–249
2. Jeppesen, M. M., Jensen, P. T., Gilså Hansen, D., Iachina, M., and Mogensen, O. (2016) The nature of early-stage endometrial cancer recurrence-A national cohort study. *Eur. J. Cancer* **69**, 51–60
3. Brooks, R. A., Fleming, G. F., Lastra, R. R., Lee, N. K., Moroney, J. W., Son, C. H., *et al.* (2019) Current recommendations and recent progress in endometrial cancer. *CA Cancer J. Clin.* **69**, 258–279
4. Wu, J., Zhang, L., Wu, S., and Liu, Z. (2022) Ferroptosis: opportunities and challenges in treating endometrial cancer. *Front. Mol. Biosci.* **9**, 929832
5. Hao, S., Yu, J., He, W., Huang, Q., Zhao, Y., Liang, B., *et al.* (2017) Cysteine dioxygenase 1 mediates erastin-induced ferroptosis in human gastric cancer cells. *Neoplasia* **19**, 1022–1032
6. Wang, H., Yang, C., Jiang, Y., Hu, H., Fang, J., and Yang, F. (2022) A novel ferroptosis-related gene signature for clinically predicting recurrence after hepatectomy of hepatocellular carcinoma patients. *Am. J. Cancer Res.* **12**, 1995–2011
7. Wang, L., Dong, L., Xu, J., Guo, L., Wang, Y., Wan, K., *et al.* (2022) Hypermethylated CDO1 and ZNF454 in cytological specimens as screening biomarkers for endometrial cancer. *Front. Oncol.* **12**, 714663
8. Huang, R. L., Su, P. H., Liao, Y. P., Wu, T. I., Hsu, Y. T., Lin, W. Y., *et al.* (2017) Integrated epigenomics analysis reveals a DNA methylation panel for endometrial cancer detection using cervical scrapings. *Clin. Cancer Res.* **23**, 263–272
9. Kulis, M., and Esteller, M. (2010) DNA methylation and cancer. *Adv. Genet.* **70**, 27–56
10. Man, X., Li, Q., Wang, B., Zhang, H., Zhang, S., and Li, Z. (2022) DNMT3A and DNMT3B in breast tumorigenesis and potential therapy. *Front. Cell Dev. Biol.* **10**, 916725
11. Chen, R., Ma, X., and Zhang, L. (2020) MicorRNA-148b inhibits cell proliferation and facilitates cell apoptosis by regulating DNA Methyltransferase 1 in endometrial cancer. *Transl. Cancer Res.* **9**, 1100–1112
12. He, D., Wang, X., Zhang, Y., Zhao, J., Han, R., and Dong, Y. (2019) DNMT3A/3B overexpression might be correlated with poor patient survival, hypermethylation and low expression of ESR1/PGR in endometrioid carcinoma: an analysis of the Cancer Genome Atlas. *Chin. Med. J.* **132**, 161–170
13. Huang, W., Li, H., Yu, Q., Xiao, W., and Wang, D. O. (2022) LncRNA-mediated DNA methylation: an emerging mechanism in cancer and beyond. *J. Exp. Clin. Cancer Res.* **41**, 100
14. He, S. L., Chen, Y. L., Chen, Q. H., Tian, Q., and Yi, S. J. (2022) LncRNA KCNQ1OT1 promotes the metastasis of ovarian cancer by increasing the methylation of EIF2B5 promoter. *Mol. Med. (Cambridge, Mass)* **28**, 112
15. Li, L., Gan, Y. P., and Peng, H. (2022) RAMP2-AS1 inhibits CXCL11 expression to suppress malignant phenotype of breast cancer by recruiting DNMT1 and DNMT3B. *Exp. Cell Res.* **416**, 113139
16. Zhang, P., Wu, S., He, Y., Li, X., Zhu, Y., Lin, X., *et al.* (2022) LncRNA-mediated adipogenesis in different adipocytes. *Int. J. Mol. Sci.* **23**, 7488
17. Yang, X., Zhao, X., Cheng, L., and Wei, R. (2021) LncRNA FOXCUT stimulates the progression of endometrial cancer. *Crit. Rev. Eukaryot. Gene Expr.* **31**, 59–66
18. Barr, J. A., Hayes, K. E., Brownmiller, T., Harold, A. D., Jagannathan, R., Lockman, P. R., *et al.* (2019) Long non-coding RNA FAM83H-AS1 is regulated by human papillomavirus 16 E6 independently of p53 in cervical cancer cells. *Sci. Rep.* **9**, 3662
19. Dou, Q., Xu, Y., Zhu, Y., Hu, Y., Yan, Y., and Yan, H. (2019) LncRNA FAM83H-AS1 contributes to the radioresistance, proliferation, and metastasis in ovarian cancer through stabilizing HuR protein. *Eur. J. Pharmacol.* **852**, 134–141
20. Kojima, K., Nakamura, T., Ooizumi, Y., Igarashi, K., Tanaka, T., Yokoi, K., *et al.* (2019) Clinical significance of cancer specific methylation of the CDO1 gene in small bowel cancer. *PLoS One* **14**, e0211108
21. Yang, Q., Wang, J., Zhong, P., Mou, T., Hua, H., Liu, P., *et al.* (2020) The clinical prognostic value of lncRNA FAM83H-AS1 in cancer patients: a meta-analysis. *Cancer Cell Int.* **20**, 72
22. Bray, F., Ferlay, J., Soerjomataram, I., Siegel, R. L., Torre, L. A., and Jemal, A. (2018) Global cancer statistics 2018: GLOBOCAN estimates of incidence and mortality worldwide for 36 cancers in 185 countries. *CA Cancer J. Clin.* **68**, 394–424
23. Wei, S., Yu, Z., Shi, R., An, L., Zhang, Q., Zhang, Q., *et al.* (2022) GPX4 suppresses ferroptosis to promote malignant progression of endometrial carcinoma *via* transcriptional activation by ELK1. *BMC cancer* **22**, 881
24. Ushijima, T., and Asada, K. (2010) Aberrant DNA methylation in contrast with mutations. *Cancer Sci.* **101**, 300–305
25. Wang, H., Peng, S., Cai, J., and Bao, S. (2021) Silencing of PTPN18 induced ferroptosis in endometrial cancer cells through p-P38-mediated GPX4/xCT down-regulation. *Cancer Manag. Res.* **13**, 1757–1765
26. Ma, F., Lei, Y. Y., Ding, M. G., Luo, L. H., Xie, Y. C., and Liu, X. L. (2020) LncRNA NEAT1 interacted with DNMT1 to regulate malignant phenotype of cancer cell and cytotoxic T cell infiltration *via* epigenetic inhibition of p53, cGAS, and STING in lung cancer. *Front. Genet.* **11**, 250
27. Zhang, H. Q., Li, T., Li, C., Hu, H. T., Zhu, S. M., Lu, J. Q., *et al.* (2022) LncRNA THOR promotes endometrial cancer progression through the AKT and ERK signaling pathways. *Med. Oncol.* **39**, 207
28. Han, C., Fu, Y., Zeng, N., Yin, J., and Li, Q. (2020) LncRNA FAM83H-AS1 promotes triple-negative breast cancer progression by regulating the miR-136-5p/metadherin axis. *Aging* **12**, 3594–3616
29. Gong, Y. B., and Zou, Y. F. (2019) Clinical significance of lncRNA FAM83H-AS1 in ovarian cancer. *Eur. Rev. Med. Pharmacol. Sci.* **23**, 4656–4662
30. Bigey, P., Ramchandani, S., Theberge, J., Araujo, F. D., and Szyf, M. (2000) Transcriptional regulation of the human DNA Methyltransferase (dnmt1) gene. *Gene* **242**, 407–418
31. Juergens, R. A., Wrangle, J., Vendetti, F. P., Murphy, S. C., Zhao, M., Coleman, B., *et al.* (2011) Combination epigenetic therapy has efficacy in patients with refractory advanced non-small cell lung cancer. *Cancer Discov.* **1**, 598–607
32. Connolly, R. M., Li, H., Jankowitz, R. C., Zhang, Z., Rudek, M. A., Jeter, S. C., *et al.* (2017) Combination epigenetic therapy in advanced breast cancer with 5-azacitidine and entinostat: a phase II national cancer institute/stand up to cancer study. *Clin. Cancer Res.* **23**, 2691–2701
33. Garafutdinov, R. R., Galimova, A. A., and Sakhabutdinova, A. R. (2019) The influence of CpG (5'-d(CpG)-3' dinucleotides) methylation on ultrasonic DNA fragmentation. *J. Biomol. Struct. Dyn.* **37**, 3877–3886
34. Meehan, R., Lewis, J., Cross, S., Nan, X., Jeppesen, P., and Bird, A. (1992) Transcriptional repression by methylation of CpG. *J. Cell Sci. Suppl.* **16**, 9–14
35. Dai, Z., Liu, X., Zeng, H., and Chen, Y. (2022) Long noncoding RNA HOTAIR facilitates pulmonary vascular endothelial cell apoptosis *via* DNMT1 mediated hypermethylation of Bcl-2 promoter in COPD. *Respir. Res.* **23**, 356
36. Song, H., Chen, L., Liu, W., Xu, X., Zhou, Y., Zhu, J., *et al.* (2021) Depleting long noncoding RNA HOTAIR attenuates chronic myelocytic leukemia progression by binding to DNA methyltransferase 1 and inhibiting PTEN gene promoter methylation. *Cell Death Dis.* **12**, 440
37. Fang, S., Gao, H., Tong, Y., Yang, J., Tang, R., Niu, Y., *et al.* (2016) Long noncoding RNA-HOTAIR affects chemoresistance by regulating HOXA1 methylation in small cell lung cancer cells. *Lab. Invest.* **96**, 60–68
38. Liang, Z., Wu, Q., Wang, H., Tan, J., Wang, H., Gou, Y., *et al.* (2022) Silencing of lncRNA MALAT1 facilitates erastin-induced ferroptosis in endometriosis through miR-145-5p/MUC1 signaling. *Cell Death Discov.* **8**, 190